International Journal of Academic Engineering Research (IJAER)
ISSN: 2643-9085
Vol. 10 Issue 5 May - 2026, Pages: 1-18

Comparative Analysis of Wear and Thermal Properties of Brake Pads Produced from Cow Hoof and Indian Bamboo Fibres

Nwosu P. C.[1]*, Arukalam I. O.[2]

[1*] Department of Mechanical Engineering, Federal Polytechnic Nekede, Owerri, Nigeria
[2] Department of Metallurgical and Material Engineering, Federal University of Technology, Owerri, Nigeria

*Corresponding Author: piusnwosu@gmail.com

Abstract: *This research presents a comparative study on the wear and thermal properties of sustainable automobile brake pads fabricated using cow hoof and Indian bamboo fibres as fillers. The fillers were processed, combined with phenolic resin, and reinforced with additives before being compression-moulded into standard brake pad specimens. Wear behaviour was evaluated using a pin-on-disc apparatus under varying loads and speeds, while thermal conductivity and stability were measured according to ASTM standards. Results showed that cow hoof-based composites exhibited lower wear rates and superior thermal resistance, while bamboo-based composites demonstrated better energy dissipation but higher wear tendency. The findings highlight the potential of combining cow hoof and bamboo fibres to optimize tribological and thermal performance for eco-friendly brake pad production.*

Keywords: Brake pads, cow hoof, Indian bamboo fibres, wear, thermal properties, sustainable composites

1. Introduction

Brake pads are composite materials made of several ingredients that work together to create friction and enable braking (Singh et al., 2023). Their main function is to convert kinetic energy into thermal energy, slowing and stopping vehicles in motion (Kumar and Suman, 2017). A typical formulation includes binders, abrasives, lubricants, reinforcing fibers, and fillers.

There are three main types of brake pads: asbestos-based, metallic, and ceramic. Asbestos pads once dominated due to good friction and thermal resistance, but they are carcinogenic (Blau, 2001). Ceramic pads generate less vibration and dust with moderate disc wear, while metallic pads provide long service life but reduce rotor lifespan (Verma, 2016; Xingming et al., 2016).

Formulations vary with desired properties but generally combine resins, fibers, friction modifiers, lubricants, and fillers to achieve characteristics like stable friction, wear resistance, and noise reduction. Common binders include epoxy or phenolic resins, while reinforcements may be ceramic, mineral, aramid, or steel fibers, along with additives such as graphite, copper powder, and metallic sulfides.

For decades, asbestos was widely used because of its excellent heat resistance, durability, and frictional properties (Moda et al., 2018). Its fibers possess high tensile strength, thermal stability up to 500 °C, flexibility, and resistance to degradation (Blau, 2001). Typically, 30–70% asbestos was incorporated into brake pads (Nicholson, 1995). It produced silicates during braking, which enhanced hardness, insulation, and wear properties (Hase & Belkar, 2015). However, inhalation of asbestos fibers during mining, processing, or repair causes severe respiratory illnesses including cancer (Swiatkowska et al., 2016). Consequently, asbestos use in brake pads has been restricted or banned in many countries due to health hazards.

The carcinogenic nature of asbestos has led to research into eco-friendly and renewable fillers (Abutu et al., 2018; Lawal et al., 2019). Several waste-based or lignocellulosic materials—including coconut shells, rice husk, palm ash, bamboo, banana peels, bagasse, maize husk, cow hooves, periwinkle shells, cocoa shells, fly ash, seashells, and lemon peel powder—have been studied as substitutes (Onyenanu et al., 2024).

Some studies combine two or more fillers in a single formulation to achieve desired physical, chemical, and tribological properties (Egeonu et al., 2015). Availability, accessibility, and performance efficiency are important considerations for adopting these sustainable fillers. The use of renewable materials aligns with global goals of reducing environmental pollution and promoting occupational safety.

Two critical indicators of brake pad performance are wear resistance and thermal properties.

Wear resistance ensures a pad withstands repeated frictional contact without excessive material loss. High wear resistance prolongs service life, reduces replacement frequency, and maintains consistent braking performance. Poor wear resistance, by contrast, compromises efficiency, safety, and vehicle reliability.

Thermal properties are equally vital. Pads must endure high braking temperatures without degrading, warping, or losing frictional stability. Excessive heat may cause brake fade, reducing stopping power. Materials with good thermal stability dissipate heat effectively, maintain consistent coefficients of friction, and resist thermal cracking or glazing.

Together, wear resistance and thermal stability ensure safety, durability, and cost-effectiveness, making them indispensable design requirements.

2. Materials and Methods

2.1 Materials for the fabrication of brake pad lining

The materials used for the production of brake pad lining and their functions are listed in Table 2.1. The choice of filler materials and other additives is justified by its availability, accessibility, affordability, as well as the health and environmental safety of the materials.

Table 2.1: The selected brake pad lining materials and justification for their choice.

Material	**Function**	**Justification for selection**
Cow hooves Bamboo	Filler	Cow hooves have been revealed to contain silicon (50.20 %), with analyses showing it as a predominant inorganic constituent within the cow hoof's composition (Bala, Okoli, Abolarin, 2016). Fastest growing plant in the world and readily available in Nigeria. Studies have shown that it has desired physical, mechanical and tribological properties for the brake pad lining development and structural design (Purboputro, Hendrawan, and Hariyanto, 2018).
Phenolic resin	Binder	Phenolic resin is a crucial component in brake pad production, acting as the primary binder that holds together various friction materials ensuring structural integrity, thermal stability, and effective braking performance. Its excellent high-temperature resistance is vital for maintaining consistent friction and preventing brake fade, while its mechanical strength and durability are essential for absorbing impact and stress during braking.
Aluminum oxide	Abrasive	Readily available and helps prevent glazing of the rotor surface, which can reduce braking efficiency.
Graphite	Friction modifier	Widely used and cheap. Burns above 700^0C. Has a high friction coefficient (0.47-0.52). Used due to its excellent lubricating properties, heat dissipation capabilities, and ability to reduce noise and vibration during braking.
Barium sulphate ($BaSO_4$)	Reinforcement	Inert, increases density, stable at high temperature and aid in wear resistance. It is used due to its high thermal stability, minimal water solubility, and low cost.

The materials in their raw state are provided as given in Plate 2.1 to Plate 2.5

Plate 2.1: Unpulverised Cow Hooves

Plate 2.2: Split lengths of Bamboo sticks

Plate 2.3: Phenolic Resin

Plate 2.4: Aluminum Oxide (Al_2O_3)

International Journal of Academic Engineering Research (IJAER)
ISSN: 2643-9085
Vol. 10 Issue 5 May - 2026, Pages: 1-18

Plate 2.5: Graphite

2.2 Equipment for the production of brake pad lining

The following equipment are used for the production of the brake pad samples:

(i) Conventional milling maching, for reducing the particle size of cow hooves and Bamboo fibres.
(ii) Thermostatic oven, for initial drying of the shredded cow hooves and Bamboo fibres.
(iii) Dessicator, for storage of samples.
(iv) Electronic weighing balance, for measurement and proportioning of samples.
(v) 100 µm Mesh sieve.
(vi) Kitchen blender, for blending and homogenization of sample materials.
(vii) Compression moulding machine, for production of brake pad samples.

2.3 Sample Preparation

2.3.1 Production of cow hooves filler and Bamboo fibre

Cow hooves were collected from Obinze abattoir, washed, sun-dried for four days, and oven-dried at 250 °C to remove oil. They were further heated in a furnace at 306 °C to eliminate volatiles, cut, crushed, and milled into powder using a ball mill. The powder was sieved with a 100 µm mesh, confirmed suitable for brake pad production (Adekunle et al., 2020; Oladokun et al., 2019).

Bamboo wood was cut, milled, ball-milled, oven-dried at 150 °C, and sieved with a 100 µm mesh to obtain fine fibres.

2.4 Characterization of the cow hooves and bamboo fibre

2.4.1 Differential Scanning Calorimetry (DSC)

A small quantity of cow hooves and bamboo were taken from the bulk sample. An empty reference pan was placed on the reference side of the DSC instrument, while the cow hoof or bamboo sample was placed in the sample pan. Thereafter, the chamber lid was closed, and the DSC control software was opened. The essential details such as the sample mass, sample name, test parameters such as start temperature, heating/cooling rates, maximum temperature and other relevant information were entered. The file name and data storage location were entered. Following the programmed inputs, the test was initiated by clicking the start button. Thus, the DSC measured the difference in heat flow required to maintain equal temperatures between the sample and reference. This data is recorded as thermograms. Hence, the melting temperature and absorbed heat energy could be determined.

2.4.2 Thermogravimetric Analysis (TGA)

The mass of each of cow hoof and and bamboo fibre sample was measured, and placed on sample pan of the thermogravimetric analyzer (TGA). The TGA instrument was programmed to heat the sample from the room temperature to 1000 ºC. The heating rate was set at 20 °C/minute. The test was initiated by clicking the start button on the TGA instrument. The TGA generated thermogravimetric curves which plotted the percentage of weight loss against the temperature. Thus, the oxidation and degradation temperatures were obtained.

2.4.3 Fourier Transform Infrared (FT-IR) Spectroscopy Analysis

The FTIR spectra of the cow hoof and bambo fillers were acquired in the range of 450–4000 cm^{-1} wavenumber by use of PerkinElmer Spectrum IR spectrophotometer, version 10.7.2. The procedure involved mixing 4 mg each of the cow hoof and bamboo sample with 100 mg of pure anhydrous KBr. The mixture was ground to fine powdered form using a mortar and a pestle. The ground mixture was then placed onto a circular disk and pressed into a transparent flake. Subsequently, it was placed into the detection chamber of

International Journal of Academic Engineering Research (IJAER)
ISSN: 2643-9085
Vol. 10 Issue 5 May - 2026, Pages: 1-18

IR spectrophotometer with a sample holder, and the IR spectra were recorded with the Omnic software at a resolution of 4 cm^{-1}, with 64 scans and a gain of 1.

2.4.4 Gas Chromatography – Mass Spectrometry (GC-MS) Analysis

The GC–MS analysis was performed using a gas chromatograph equipped with a autosampler and a mass-selective detector (Agilent, Santa Clara, CA, USA). The capillary column used was HP-5MS, 30 m × 0.25 mm × 0.25 mm, from Agilent (Santa Clara, CA, USA). Helium was used as carrier gas at 1.5 mL/min. The split–splitless injector was operated in pulsed pressure splitless mode as follows: initial pressure 0.2 MPa (30 p.s.i.) for 1.3 min, decreased to constant flow. The purge valve was opened after 1.5 min. The injection volume was 5 µL. The temperatures of the GC system were set as follows: injector temperature 290 °C; transfer line temperature 280 °C; oven temperature program: 50 °C (1.5 min)–30 °C/min–180 °C–20 °C/min–280 °C (20 min). MS detector (quadrupole) was operated in the EI mode at 70 eV with a mass scan range of 50–450 m/z and the sampling rate of 3.6 scans/s.

2.5 Production of the brake pad samples

The brake pad samples production was based on the formulation given in Table 2.2.

Table 2.2: The formulations for brake pad samples production (% Weight)

Sample ID / Materials	01	02	1	2	3	4	5	6	7
Cow hooves filler (%wt.)	10	-	8	7	6	5	4	3	2
Bambo fibre (%wt.)	-	10	2	3	4	5	6	7	8
Phenolic Resin (%wt.)	70	70	70	70	70	70	70	70	70
Aluminum Oxide (%wt.)	5	5	5	5	5	5	5	5	5
Graphite (%wt.)	5	5	5	5	5	5	5	5	5
Barium Sulphate (%wt.)	10	10	10	10	10	10	10	10	10

Where
01 = Formulation without bamboo fibre;
02 = Formulation without cow hooves filler;
1 – 7 = Formulations with varying amounts of cow hooves filler and bamboo fibre

Each sample formulation was prepared and compression-molded at a mold temperature of 130 ºC and clamping pressure of 100 psi using a compression molding machine. After compression-molding, each sample was post-cured for 5 minutes. Thereafter, the fabricated brake pad samples were removed and air-dried for 2 hours before they were kept in the desiccator prior to characterization.

Plate 2.6 The fabricated brake pad samples

2.6 Thermal properties and wear tests

International Journal of Academic Engineering Research (IJAER)
ISSN: 2643-9085
Vol. 10 Issue 5 May - 2026, Pages: 1-18

2.6.1 Thermal conductivity

The brake pad sample was cut into a rectangular form to fit the testing apparatus. The sample was conditioned at room temperature and humidity to ensure it was free of moisture and contaminants that might affect the test results. The steady-state heat flow method using a thermal conductivity meter was used. The apparatus was calibrated using reference materials with known thermal conductivity values to ensure accuracy. The test was performed at a controlled temperature, often close to the operating temperature range of the brake pad lining (e.g., 25°C to 300°C). A controlled heat source was applied to one side of the brake pad lining sample, while the opposite side was kept at a lower temperature by cooling.

The temperatures on both sides of the sample were measured accurately using thermocouples. The temperature difference (ΔT) between the hot and cold sides was recorded. The amount of heat passing through the sample (Q) was measured. In a steady-state condition, the heat flow remains constant over time. The thickness of the brake pad lining sample (d) was measured accurately, as it is a crucial factor in calculating thermal conductivity. Using Fourier's law of heat conduction, the thermal conductivities (k) were calculated thus;

$$\mathrm{k} = \frac{Q.d}{A.\Delta T} \tag{2.1}$$

Where Q = Heat flow through the sample (W), d = Thickness of the sample (m), A = Cross-sectional area of the sample through which heat flows (m^2), ΔT = Temperature difference across the sample (K). Thus, the thermal conductivity is expressed in units of W/m·K (watts per meter per degree Kelvin).

2.6.2 Melting Temperature using Differential Scanning Calorimetry (DSC)

A small, representative brake pad sample was cut out from the bulk sample. An empty reference pan was placed on the reference side of the instrument, while the brake pad sample was placed in the sample pan. After that, the chamber lid was closed. Then, the DSC control software was opened, and the essential details such as the sample mass, sample name, test parameters such as start temperature, heating/cooling rates, maximum temperature and other relevant information were entered. The file name and data storage location were entered. Following the programmed inputs, the test was initiated by clicking the start button. Thus, the DSC measures the difference in heat flow required to maintain equal temperatures between the sample and reference. This data were recorded as thermograms. Hence, the melting temperature and absorbed could be determined.

2.6.3 Wear rate test

The wear rate was determined by adopting the method by Hanni, Khaira, and Esthar (2011). According to this method, each sample was clamped rigidly in position along the disc of the grinding machine for 60 seconds. The weight of each of the samples was measured before and after grinding. The difference in weight after the grinding process indicate the loss in weight. Knowing the speed of the grinding machine and its disc diameter, the wear rate (W_r) was calculated thus:

$$Wr = \frac{\Delta \mathrm{W}}{2\pi NRt} \tag{2.2}$$

Where ΔW = weight loss (g), R = radius of grinding disc (cm), N = speed in rpm (revolution per minute), t = time of grinding (i.e. 60 s).

3. Results

3.1 Thermal properties of cow hoof filler.

3.1.1 Differential scanning calorimetry (DSC) and thermogravimetric analyses (TGA)

Results of the differential scanning calorimetry (DSC) and thermogravimetric analyses (TGA) conducted on the pulverized cow hooves filler are presented in Figure 3.1. Also, the results of the TGA analysis of the pulverized cow hooves are given in Figure 3.2. The TGA results are plotted separated to clearly define the decomposition steps.

International Journal of Academic Engineering Research (IJAER)
ISSN: 2643-9085
Vol. 10 Issue 5 May - 2026, Pages: 1-18

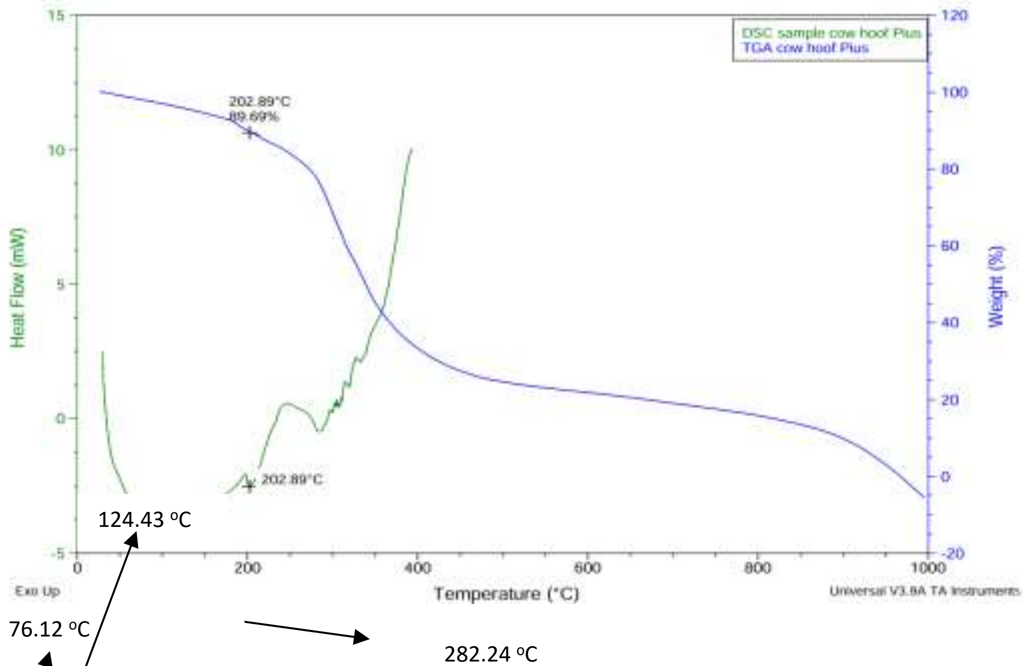

Figure 3.1: DSC and TGA results for pulverized cow hooves

The DSC and TGA analyses were undertaken to enable determination of the melting and decomposition temperatures. The determination of these two temperature profiles is very important as it helped assess the purity of the cow hooves and their behaviour under heat. The melting temperature via DSC helped to identify the crystallinity of the cow hooves, while decomposition temperature obtained via TGA helped to provide insight into the thermal stability of the cow hooves. Overall, knowledge of the melting and decomposition temperatures helped to determine the fabrication temperature of the brake pad lining.

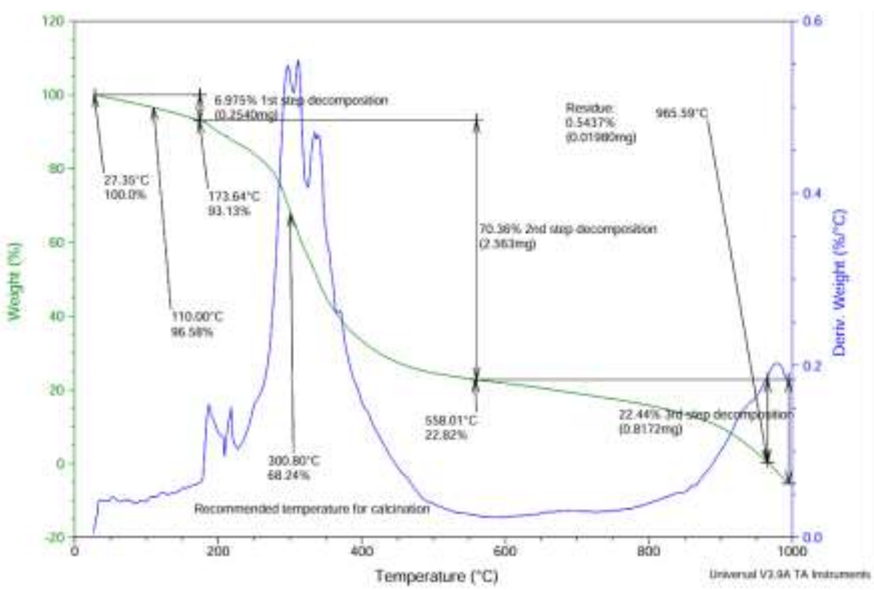

Figure 3.2: TGA results for pulverized cow hooves

3.1.2 Fourier Transform Infrared (FT-IR) spectroscopy

The FT-IR spectra of the cow hooves filler are presented in Figure 3.3.

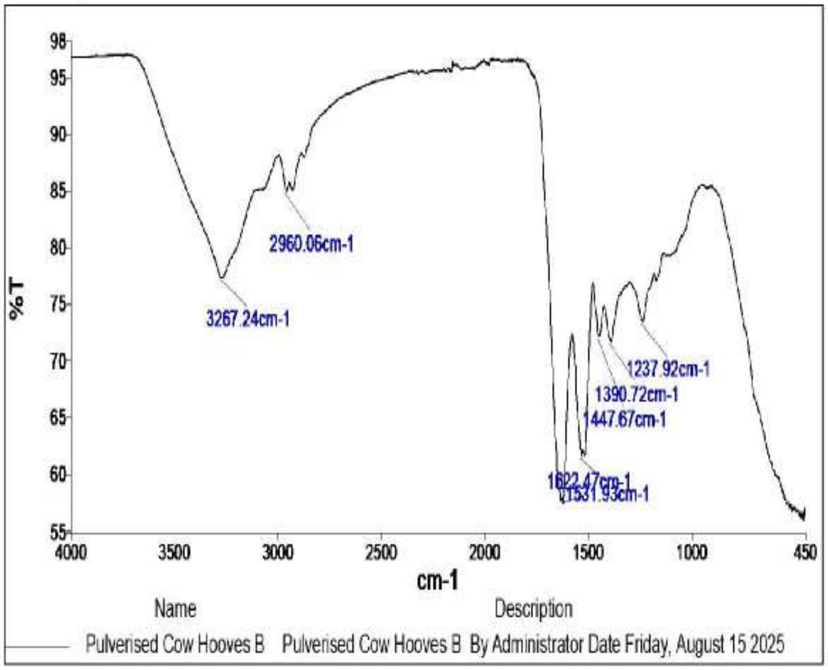

Figure 3.3: FT-IR spectra of pulverized cow hooves

The FTIR spectra of cow hooves in Figure 3.3 show prominent absorption peaks corresponding to the proteinaceous keratin material, with characteristic absorption band values listed in Table 3.1.

Table 3.1: FT-IR absorption bands of the cow hooves

Peak Number	**Wavenumber (cm^{-1})**	**Transmittance (%T)**
1	3267.24	77.39
2	2960.06	85.09
3	1622.47	57.36
4	1531.93	61.57
5	1447.67	72.19
6	1390.72	71.77
7	1237.92	73.51

3.1.3 Gas Chromatography – Mass Spectrometry (GC-MS)

The GC-MS results of the cow hooves are graphically depicted in Figure 3.4

International Journal of Academic Engineering Research (IJAER)
ISSN: 2643-9085
Vol. 10 Issue 5 May - 2026, Pages: 1-18

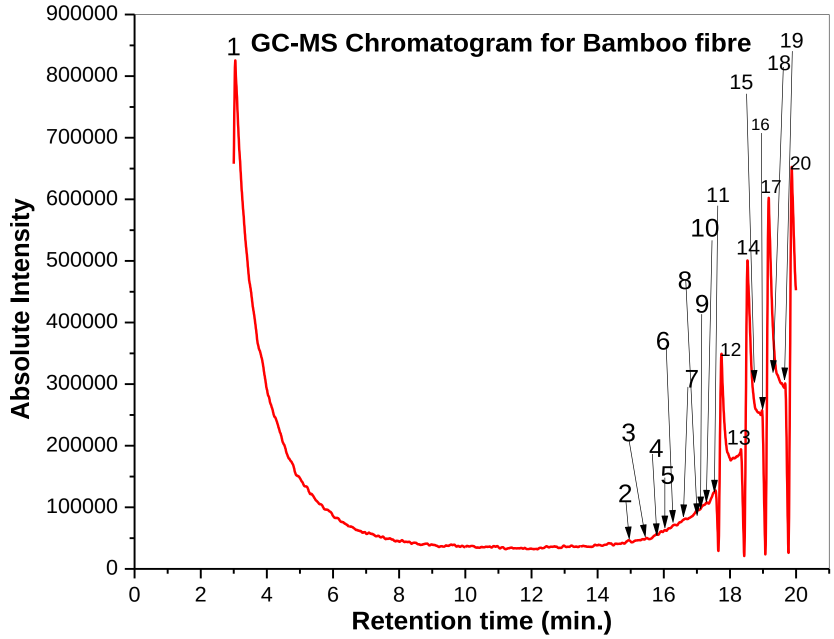

Figure 3.4: GC-MS chromatogram of pulverized cow hooves

The GC-MS chromatogram of pulverized cow hooves in Figure 3.4 revealed prominent peaks corresponding to the composition of the cow hooves, and the areas of the peaks with the names of constituent materials are listed in Table 3.2.

Table 3.2: GC-MS peak report for the cow hooves

Peak #	Retention time (min.)	Area	Name of constituent
1.	3.041	2594244	2-Aminoimidazole-5-propionic acid
2.	5.566	21602	1,1,1 -Trifluoro-2-propanol
3.	6.573	22051	2-Octanol, (S) -
4.	7.326	17175	3-Nonyn – 1 – ol
5.	9.829	27858	3-(Methylthio) pent-4-yn-1-ol
6.	10.897	26254	6,9,12-Octadecatrien-1-ol
7.	13.390	20751	Cyclohexanone, O-methyloxime
8.	14.265	23476	Gentamicine a
9.	15.000	124948	Trycyclo [5.1.0.0(3,5)]octane-2, 6-dione, 1,3,5,7-tetramethyl -
10.	15.206	174525	Glutaric acid, 3-(2-methoxyethyl)nonyl propyl ester
11.	15.438	387967	Octanamide, N –(2 -mercaptoethyl) -
12.	15.550	227403	2-Butenoic acid, 2-methyl-, 4,4a, 5, 6, 7, 8, 8a,9-octahydro-8a-hydroxy-3,4a,5-trimethylnaphthol[2,3-b]furan-6-yl ester
13.	15.985	1413263	2-Oxa-7-thiatricyclo[4.4.0.0(3,8)]decane
14.	16.195	1124798	8-Chloro-8-methyl-cis-8-silabicyclo[4,3,0]nonane
15.	16.380	957411	1,3-Benzodioxole, 5-[1-[2-(2-butoxyethoxy)ethoxy]butyl]-
16.	16.550	1072462	Undecane, 1,2,-dibromo-2-methyl-
17.	17.999	26709755	Spiro[androst-5-ene -17 ,1'-cyclobutane]-2'-one, 3-hydroxy-, (3.beta.,17.beta)-
18.	18.398	23514158	Ethy iso-allocholate
19.	18.982	9696729	Spiro [androst-5-ene-17,1'-cyclobutan]-2'-one, 3-hydroxy- , (3.beta., 17.beta)-
20.	19.302	19274091	Spiro [androst-5-ene-17,1'-cyclobutan]-2'-one, 3-hydroxy- , (3.beta., 17.beta)-

International Journal of Academic Engineering Research (IJAER)
ISSN: 2643-9085
Vol. 10 Issue 5 May - 2026, Pages: 1-18

3.2 Bamboo fibre

After shredding of the bamboo wood, the fibres obtained are presented.

3.2 Thermal properties of bamboo filler

3.2.1 Differential scanning calorimetry (DSC) and thermogravimetric analysis (TGA)

The thermal analyses of the bamboo fibre via differential scanning calorimetry (DSC) and thermogravimetric analysis (TGA) are shown in the thermograms given in Figure 3.5.

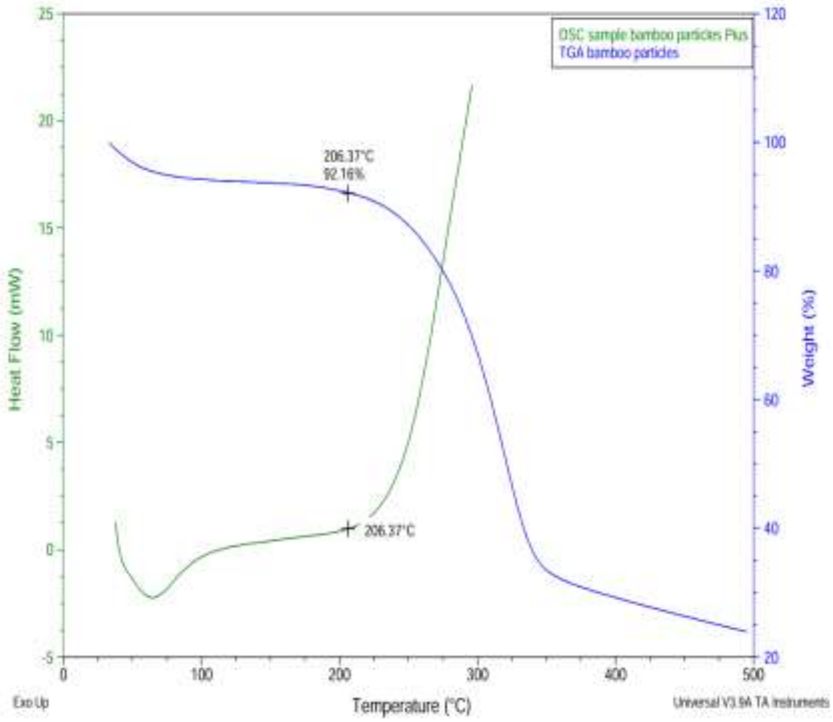

Figure 3.5: DSC and TGA results for shredded bamboo fibres

As earlier stated in the case of cow hooves, the DSC and TGA analyses were undertaken to enable determination of the melting and decomposition temperatures of the bamboo fibres. The DSC determination of the melting temperature of bamboo fiber is important for optimizing its processing and application in composites.

For in-depth analysis on the decomposition of the bamboo fibre, the TGA thermogram was plotted separately to clearly reveal the steps involved in the decomposition of the bamboo fibre. This is presented in Figure 3.6.

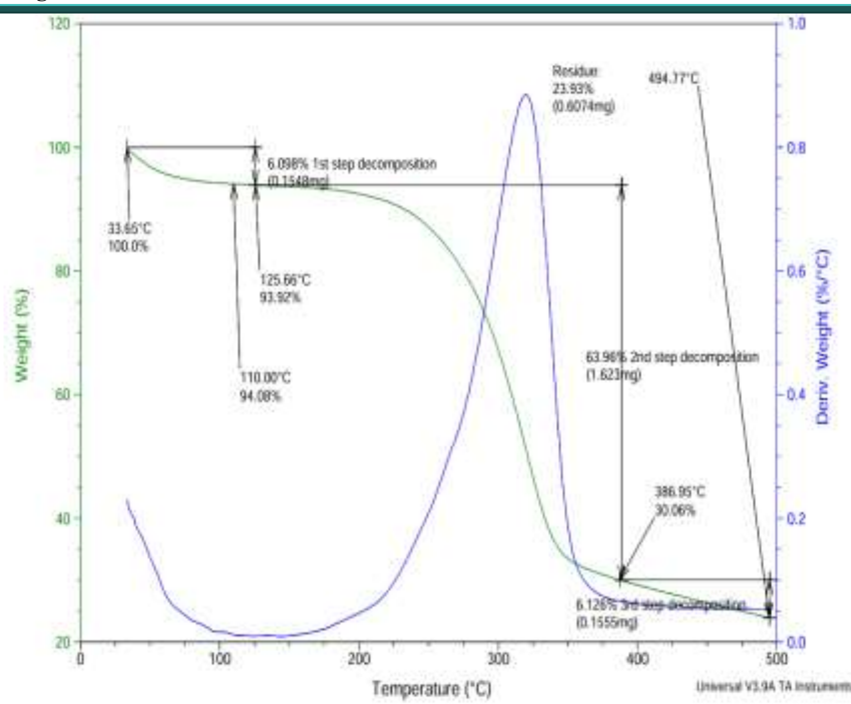

Figure 3.6: TGA results for shredded Bamboo fibres

The TGA determination of the decomposition temeperature helps to understand the thermal stability and degradation behavior of bamboo fibres. This knowledge allows for the proper selection of processing temperature of the brake pad lining to avoid degradation of the enmeshed fiber, and to maximize the desired properties of the final product, such as strength and modulus.

3.2.2 Fourier Transform Infrared (FT-IR) spectroscopy

The FT-IR spectra of the bamboo filler are presented in Figure 3.7. From the Figure 4.7, the absorption peaks and the corresponding wavenumbers are clearly revealed.

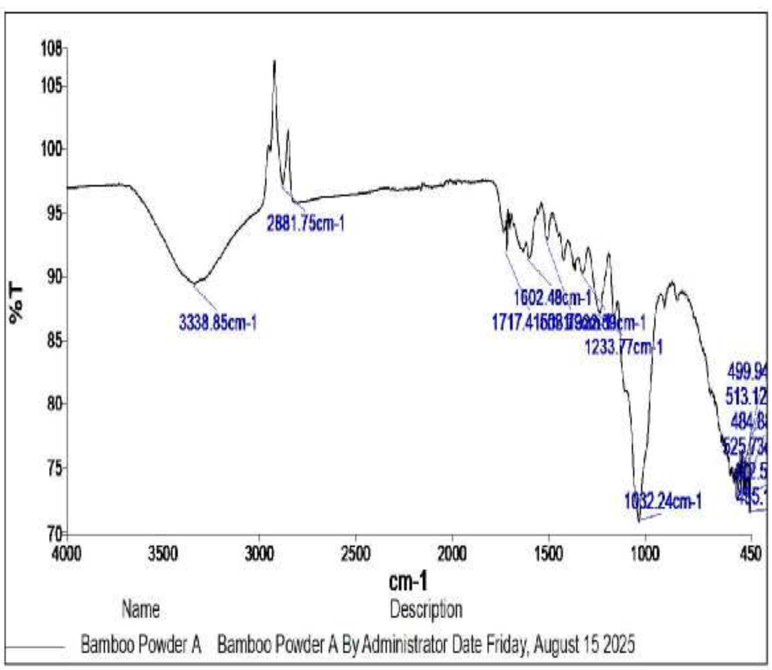

Figure 3.7: FT-IR spectra of pulverized bamboo powder

International Journal of Academic Engineering Research (IJAER)
ISSN: 2643-9085
Vol. 10 Issue 5 May - 2026, Pages: 1-18

The FT-IR absorption values extracted from the Figure 3.7 are listed in Table 3.3.

Table 3.3: FT-IR peak absorption values

Peak Number	Wavenumber (cm^{-1})	Transmittance (% T)
1	3338.85	89.50
2	2881.75	97.29
3	1717.41	92.14
4	1602.48	91.55
5	1503.79	92.97
6	1322.59	90.37
7	1233.77	87.16
8	1032.24	70.70
9	525.73	72.57
10	51312	73.08
11	499.94	73.45
12	484.88	72.81
13	472.57	72.53
14	455.11	71.43

3.2.3 Gas Chromatography – Mass Spectrometry (GC-MS)

The GC-MS results of the bamboo filler are presented in Figure 3.8

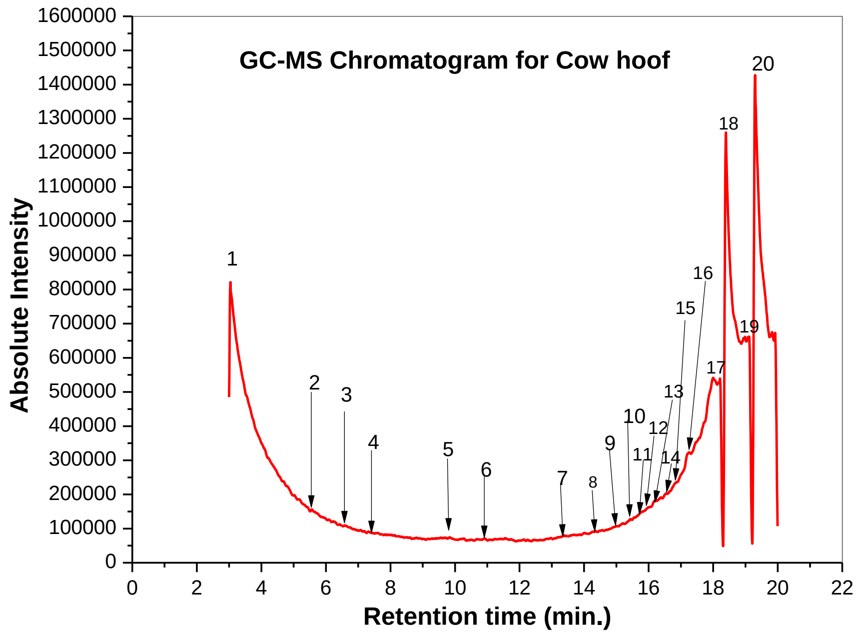

Figure 3.8: GC-MS chromatogram of pulverized bamboo fibres

The GC-MS chromatogram of pulverized bamboo fibres in Figure 3.8 revealed prominent peaks corresponding to the composition of the bamboo fibres, and the areas of the peaks with the names of constituent materials are listed in Table 3.4.

Table 3.4: GC-MS peak report for the bamboo fibres

Peak #	**Retention time (min.)**	**Area**	**Name of constituent**
1.	3.045	1015478	2-Pentene, 4-Bromo-
2.	14.935	27102	Pentanedioic acid, 3-thioxo-, diethyl ester
3.	15.915	17196	Cycloheptanol, 2-chloro-, trans-

4.	16.025	9494	Acetamide, 2-(4-morpholylcarbonylmethyl)thio-N-phenyl-
5.	16.150	12362	1-[N-Aziridyl]propane-2-thiol
6.	16.285	23951	Cycloheptanol, 2-chloro-, trans-
7.	16.475	6718	1-Octanesulfonyl chloride
8.	17.010	211725	Acetamide, N-methyl-N-[4-[4-fluoro-l-hexahydropyridyl]-2-butynyl]-
9.	17.195	319547	2-Hydoxyethyl hydrogen vinyphosphonate
10.	17.300	376573	4H-Thiopyran-4-one, 1,1-dioxide
11.	17.566	1150768	1,3,5-Triazine-2,4-diamine, N,N'-bis(1-methylethyl)-6-(methylsulfonyl)-
12.	17.743	2569215	Spiro[androst-5-ene-17, 1'-cyclobutan]-2'-one, 3-hydroxy-, (3.beta., 17.beta.)-
13.	18.332	502808	Spiro[androst-5-ene-17, 1'-cyclobutan]-2'-one, 3-hydroxy-, (3.beta., 17.beta.)-
14.	18.531	7450540	3-Methyl-4-(phenythio)-2-prop-2-enyl-2,5-dihydrothiophene 1,1-dioxide
15.	18.895	1102011	4-Benzylpiperidine
16.	18.971	1147891	2,3-O-Benzal-d-mannosan
17.	19.172	9976931	3-Methyl-4-(phenythio)-2-prop-2-enyl-2,5-dihydrothiophene 1,1-dioxide
18.	19.570	1470076	2,4-Dinitro-4'-methoxydiphenylsulfone
19.	19.670	1242834	Tetraacetyl-d-xylonic nitrile
20.	19.868	2675749	[1,1'-Bicyclopropyl]-2-octanoic acid, 2'hexyl-, methyl ester

3.3 Thermal properties of the fabricated brake pad samples

3.3.1 Thermal conductivity

The thermal conductivities of the brake pad linings were determined to understand how they transfer heat, which is crucial for energy efficiency and safety of the brake pad linings. Thus, the thermograms obtained for the thermal conductivities of the brake pad samples using DSC technique are given in the Appendix 1. Consequently, the extracted values of the thermal conductivities of the nine (9) samples of the brake pad are presented in Table 3.5.

Table 3.5: Thermal Conductivity values for the fabricated brake pad linings

Sample ID	01	02	1	2	3	4	5	6	7
T_C, $W\cdot mm^{-1}\cdot K^{-1}$	0.0091	0.0142	0.0108	0.0079	0.0111	0.0086	0.0091	0.0084	0.0116

For clarity and better understanding, these results are graphically presented in Figure 3.11.

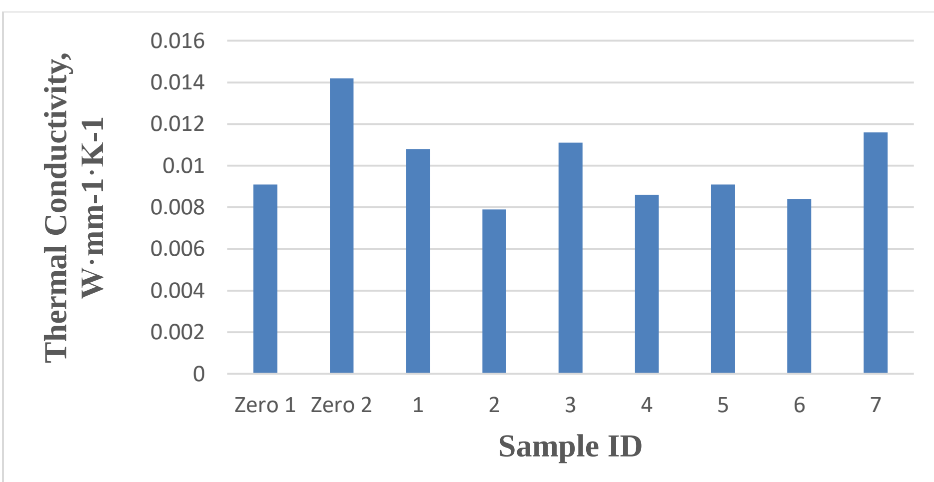

International Journal of Academic Engineering Research (IJAER)
ISSN: 2643-9085
Vol. 10 Issue 5 May - 2026, Pages: 1-18

Figure 3.11: Plot of thermal conductivities of the fabricated brake pad samples

3.3.2 Melting temperature

The melting temperatures (Tm) of the brake pad samples were determined from the differential scanning calorimetry (DSC) curves. They were determined by identifying the peaks of endothermic events on the thermograms. Therefore, the melting point is the temperature at which the sample absorbs heat without a change in its own temperature, known as the latent heat of fusion, and this absorption appears as an endothermic peak on the DSC curve. Hence, the melting temperatures of the brake pad samples are given in Table 3.6.

Table 3.6: Melting temperatures for the fabricated brake pad linings

Sample ID	01	02	1	2	3	4	5	6	7
Tm, K	340.48	340.42	340.01	340.00	341.61	340.86	340.46	340.87	341.50
Tm, ºC	67.33	67.27	66.86	66.85	68.46	67.71	67.31	67.72	68.35

For better understanding of the trend, the melting temperatures of the fabricated brake pad samples are depicted in Figure 3.12.

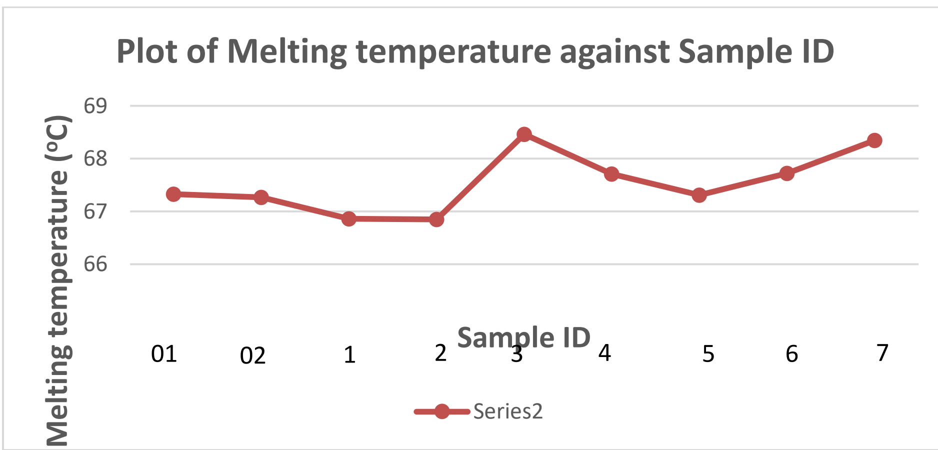

Figure 3.12: Melting temperature for the fabricated brake pads

3.4 Wear rate

Wear rate testing on brake pads is crucial for evaluating their lifespan and performance. It involves measuring material loss over time. The test is vital for assessing the durability and performance of the brake pads. The test also helps to ensure vehicle safety and efficiency, especially in response to environmental and regulatory demands. The results of the wear rate test conducted on the brake pad samples are given in Table 3.13.

Table 3.13: Values of wear rate test for the fabricated brake pad samples

Sample ID	01	02	1	2	3	4	5	6	7
Wear Rate, g/m.	2.504E-08	1.952E-08	1.704E-08	1.391E-08	1.387E-08	2.047E-08	2.091E-08	1.798E-08	1.026E-08

The wear rate values for the fabricated brake pad samples are depicted in Figure 3.24 for better understanding.

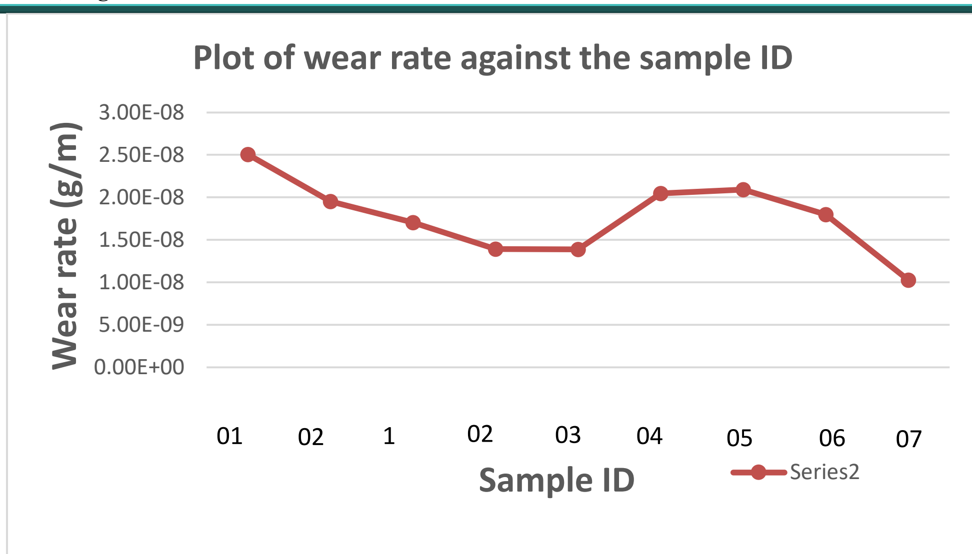

Figure 3.24: Plot of wear rate versus sample ID

4. Discussion

4.1 Effect of varying proportion of cow hoof and bamboo fibre on the thermal properties and wear resistance of the fabricated brake pads.

4.1.1 Thermal Conductivity

The thermal conductivity test for brake pad linings is a critical evaluation that determines how well a brake pad lining material can conduct heat. Understanding the thermal conductivity of a brake pad lining is also essential for assessing its ability to dissipate the heat generated during braking, which affects the overall performance and safety of the braking system. The thermal conductivity test measures the rate at which heat flows through the brake pad lining material. Since brake pad linings are subjected to intense heat due to friction during braking, high thermal conductivity is often desirable to prevent excessive temperature buildup, which can lead to brake fade, reduced friction, and even failure of the braking system.

High thermal conductivity indicates that the brake pad lining material can efficiently dissipate heat, reducing the risk of overheating, brake fade, and thermal damage to the braking system. Low thermal conductivity indicates that the brake pad lining material retains more heat, which could lead to higher operating temperatures and potential degradation of the brake pad lining material under extreme conditions.

In view of these established knowledge, the thermal conductivity values for the fabricated brake pad linings as given in Table 3.5 and graphically depicted in Figure 3.11 show that the brake pad sample containing only bamboo fibre as filler exhibited the highest thermal conductivity of 0.0142 $W{\cdot}mm^{-1}{\cdot}K^{-1}$, whereas the brake pad sample containing only cow hoof as filler has a lower thermal conductivity of 0.0091 $W{\cdot}mm^{-1}{\cdot}K^{-1}$. This implies that the brake pad sample containing only the bamboo fibre as filler material would dissipate heat better than the brake pad sample with cow hoof as filler material. The reason is that bamboo fibre inherently has a higher thermal conductivity than cow hoof, leading to better heat dissipation and resistance to heat-related performance issues. Additionally, the high carbon content and cellular structure of the bamboo fibre, allows for more efficient transfer of heat, whereas cow hoof which has porous structure is less effective at conducting heat.

Considering the effect of varying proportion of cow hoof and bamboo fibre on the thermal conductivity of the fabricated brake pad samples, it was observed that the brake pad sample 7 containing highest amount of bamboo fibre exhibited highest thermal conductivity. The reason is as earlier mentioned that bamboo fibre has a higher thermal conductivity than cow hoof.

4.1.2 Melting temperature

The values of melting temperature of the fabricated brake pad samples as given in Table 3.6 and graphically depicted in Figure 3.12 show that the brake pad sample with only cow hoof revealed a melting temperature of 67.33 ^oC slightly higher than 67.27 ^oC which is the melting temperature of the brake pad sample containing only bamboo fibre. Further, considering the combined effect of cow hoof and bamboo fibre, sample 3 with higher amount of cow hoof compared to bamboo fibre exhibited the highest melting

International Journal of Academic Engineering Research (IJAER)
ISSN: 2643-9085
Vol. 10 Issue 5 May - 2026, Pages: 1-18

temperature of 68.46 ºC. The reason is that cow hoof melted at 202.89 °C whereas bamboo fibre and phenolic resin do not have melting temperatures but degrade at elevated temperatures.

Moreso, it is an established fact that a brake pad's melting temperature depends on the inherent thermal stability of its constituent materials and binders, and not the specific material itself. In as much as cow hoof has demonstrated to have higher thermal resistance than bamboo fibres which has relatively low thermal stability, the overall thermal stability of the fabricated brake pad samples was observed to be a function of the amount of cow hoof, and presence of phenolic resin as binder plus other constituent materials.

However, it could be observed that the melting temperatures of the brake pad samples are quite lower than the cow hoof. The constituent materials in the brake pad formulation, particularly the lubricant reduced the molecular mobility of the cow hoof structure, and thus the melting temperature significantly reduced.

4.1.3 Wear rate

The wear rate test for brake pad linings is a crucial assessment used to determine the durability and longevity of brake pad linings under simulated conditions of friction and heat. This test provides insights into how much material is lost from the brake pad lining during braking, which directly correlates to the lifespan of the brake component. The wear rate test is designed to quantify the material loss of a brake pad lining when subjected to frictional forces. The rate of wear is critical for understanding how long a brake lining will last under normal operating conditions and how often it will need to be replaced. A low wear rate indicates that the brake lining material is durable and will have a longer service life, whereas a high wear rate suggests that the material may degrade quickly, necessitating more frequent replacements. The wear rate data is essential for predicting the maintenance intervals for brake systems and ensuring safety in vehicle operation.

Hence, Table 3.13 presents values of wear rate test for the fabricated brake pad samples. The data are presented graphically in Figure 3.24 for better understanding of the trend with respect to addition of both cow hoof and bamboo fibres. From the given results, the brake pad sample 01 with only cow hoof as filler material gave highest vaue of wear rate (2.504E-08 g/m) compared to the sample 02 with only bamboo fibre as filler material which gave the value of 1.952E-08 g/m.
Considering the effect of varying proportion of cow hoof and bamboo fibre, sample 7 with higher proportion of bamboo fibre than cow hoof gave the lowest wear rate (1.026E-08 g/m), suggesting that the brake pad sample would be most durable with the longest service life compared to other samples.

The reason the brake pad sample with higher proportion of bamboo fibre exhibit lower wear rate is due to the fibrous nature of bamboo which allows it to create more coherent and stable wear layers plus the inherent structural characteristics of bamboo fibre, which include higher mechanical properties, better durability, and a greater capacity for forming stable frictional contact surfaces with the brake disc. Whereas the sample with high proportion of cow hoof display higher wear rate because the organic composition of cow hoof is more prone to fragmentation, leading to higher rates of wear particle generation and a less durable friction interface.

5. Conclusion

This study was conducted with the main objective of comparative analysis of wear and thermal properties of brake pads produced from cow hoof and Indian bamboo fibres. The brake pad samples were produced using some selected materials. Consequently, they were characterized as required. Thus, the following conclusions were drawn.

(i) The result of the characteristic thermal events of the pulverized cow hooves determined using the DSC revealed a denaturation temperature around 76.12°C. An endothermic peak observed at 202.89 °C represents the melting temperature of the crystalline silicon and a few other crystalline mineral elements in the cow hoof. Again, another sharp endothermic peak was observed at 282.24 °C which is linked to the cleavage of disulfide bonds in the cow hoof.
The TGA analysis showed the first step decomposition occurred at temperatures between 27.35 and 173.64 °C, whereas the second decomposition temperature occurred at the temperatures between 173.64 and 558.1°C where thermal breakdown of keratin, which is the main component of cow hoof that is rich in sulfur and amino acids occurred. Further, at temperature ranging from 558.1 to 965.59 °C, carbonization occurred (i.e. the third step decomposition).
FT-IR characterization of cow hooves revealed presence of N-H, C=O, and C-N groups which indicate presence of peptide bonds in raw cow hoof and keratin. Further, GC-MS analysis of the cow hooves revealed presence of hydrocarbons, carboxylic acid, alkanols, esters, and ketone compounds in the cow hooves, and therefore confirms that cow hoof has self-lubricating oils which could help in the operation of brake pads.

Similarly, the FT-IR test results for the pulverized bamboo fibre shows presence of absorption peaks which are linked to O–H, C–H, C–O, C=O, C=C groups present in cellulose, hemicellulose, and lignin of bamboo fibres. The GC-MS analysis of bamboo fibres revealed presence of some volatile chemical compounds which belong to the family of alkanols, acids, esters, aldehydes, and ketones, and therefore testifies that bamboo fibre has the capacity for self-lubricating functionality.

(ii) Nine (9) different brake pad samples where successfully produced using each of cow hoof and bamboo fibres as filler mterials. Further, the combination of cow hoof and bamboo fibres were used as filler materials in the fabrication of the brake pad samples. Consequently, the average thickness of the brake pad samples fabricated were determined to be 5.80 mm.

(iii) Considering the effect of varying proportion of cow hoof and bamboo fibre on the thermal conductivity of the fabricated brake pad samples, it was observed that the brake pad sample 7 containing highest amount of bamboo fibre exhibited highest thermal conductivity. When considered the combined effect of cow hoof and bamboo fibre on the melting temperature of the fabricated brake pad samples, sample 3 with higher amount of cow hoof compared to bamboo fibre exhibited the highest melting temperature of 68.46 ^{o}C.

(iv) With respect to wear rate determination, sample 7 with higher proportion of bamboo fibre than cow hoof gave the lowest wear rate (1.026E-08 g/m), suggesting that the brake pad sample would be most durable with the longest service life compared to other samples.

6. References (Samples in Elsevier/APA Style)

References

Abdulrahman, A.S., Ajani, C.K., Aliyu S.A. (2021). Production and characterization of asbestos-free brake lining material using agro wastes. *Engineering and Applied Science Research* 2021;48(4):379-384

Abutu J., Lawal S.A., Ndaliman M.B., Lafia-Araga R.A., Adedipe O., Choudhury I.A. Effects of process parameters on the properties of brake pad developed from seashell as reinforcement material using grey relational analysis, *Eng. Sci. Tech., Int. J.* 2018, https://doi.org/10.1016/j.jestch.2018.05.014.

Abutu J., Lawal S.A., Ndaliman M.B., and Lafia-Araga R.A. An overview of brake pad production using non-hazardous reinforcement materials. *Acta Technica Corviniensis*, 2018, 143-156.

Adams, D. R. 8-Tribological considerations in internal combustion engines . In *Tribology and Dynamics of Engine and Powertrain*, Woodhead Publishing, 2010; 251-283. https://doi.org/10.1533/9781845699932.2.251.

Adekunle, N. O., Oladejo, K. A., Abu, R., Oriolowo, K. T., Ismaila, S. O., & Adegboyega, S. M. Characterisation of Asbestos-Free Brake Pad . *International Journal of Scientific & Engineering Research*, 2020, 11(5),193-198.

Ademoh , A. N., & Adeyemi , I. O. Development and Evaluation of Maize Husks (Asbestos-Free) Based Brake Pad . *International Institute for Science, Technology and Education (IISTE), Industrial Engineering Letters –IEL*, 2015, 5(2), 67 –80.

Adetunji O.R., Adedayo A.M., Ismailia S.O., Dairo O.U., Okediran I.K., Adesusi O.M. Effect of silica on the mechanical properties of palm kernel shell based automotive brake pad. *Mechanical Engineering for Society and Industry*, 2022; 2(1):7-16. https://doi.org/10.31603/mesi.6178.

Adeyemi, I. O., Nuhu, A. A., & Thankgod, E. B. Development of Asbestos-Free Automotive Brake Pad Using Ternary Agro-Waste Fillers. *Journal of Multidisciplinary Engineering Science and Technology*, 2016, *3* (7), 5307-5323.

Bala, K. C., Okoli, M., & Abolarin, M. S. Development of automobile brake lining using pulverized cow hooves. *Leonardo Journal of Sciences*, 2016, 95-108.

Crăciun A.L., Pinca-Bretotean C., Baneasa C.B., Josan A. Composites materials for friction and braking application, *IOP Conference Series Materials Science and Engineering*, 2017, 200(1):012009. DOI: 10.1088/1757-899X/200/1/012009.

Dhakal H.N., Zhang Z.Y., and Richardson M.O.W. Effect of Water Absorption on the Mechanical Properties of Hemp Fibre Reinforced Unsaturated Polyester Composites. *Composites Science and Technology*, 2007; 67:1674-1683.

Egeonu, D., Oluah, C., & Okolo, P. Production of eco-friendly brake pad using raw materials sourced locally in Nsukka. *Journal of Energy Technologies and Policy*, 2015, 5(11),47-54.

Eriksson, M., & Jacobson, S. Tribological surfaces of organic brake pads. *Tribal. Intern*, 2000, 33, 817-827.

Furuya, S., Chimed-Ochir, O., Takahashi, K., David, A., & Takala, J. Global Asbestos Disaster. *Int. J. Environ. Res. Public Health* , 2018, 15,1000, 1-18.

Gawande S. H., Banait A. S. and Balashowry K. Study on wear analysis of substitute automotive brake pad materials, Australian Journal of Mechanical Engineering, 2020, DOI:10.1080/14484846.2020.1831133.

Han, X. An investigation into the tribological property of coatings on micro- and nanoscale. In *Anti-Abrasive Nanocoatings.* 2015.

Hanni, A. A., Khaira, H. S., & Esthar, M. M. Effect of loads sliding speeds and times on the wear rate. *American Journal of Scientific and Industrial Research*, 2011, 2(1), 99-106.

Ige O.E., L. Inambao F.L. and Adewumi G.A. Effects of Fiber, Fillers and Binders on Automobile Brake Pad Performance: A Review. *International Journal of Mechanical Engineering and Technology*, 2019, 10(6): 135-150.

Ige O.E., Inambao F.L., and Adewumi G.A. Biomass-Based Composites For Brake Pads: A Review. *International Journal of Mechanical Engineering and Technology (IJMET),* 2019; 10(3):920–943

Kakkar P., Madhan B., and Shanmugam G., Extraction and characterization of keratin from bovine hoof: a potential material for biomedical applications, *SpringerPlus*. (2014) 3(1), https://doi.org/10.1186/2193-1801-3-596, 2-s2.0-84933053814.

Kauppinen, T., & Korhonen, K. Exposure to Asbestos During Brake Maintenance of Automotive Vehicles by Different Methods. *American Industrial Hygiene Association Journal*, 2010. 48(5), 499-504.

Kumawat T.K., Sharma A., Sharma V., and Chandra S., Keratin Waste: The Biodegradable *Polymers*, (2018), Intech Open, Keratin. DOI: 10.5772/intechopen.79502.

Lemen, R. A. Asbestos in Brakes: Exposure and Risk of Disease. *American Journal of Industrial Medicine*, 2004, 45, 229–237.

Li L-J., Wang Y-P., Wang G., Cheng H-T., Han X.-J. Evaluation of properties of natural bamboo fiber for application in summer textiles. Journal of Fiber Bioengineering and Informatics. 2010;3(2):94-99.

Mayowa, A., Abubakre, O. K., Lawal, S. A., & Abdulkabir, R. Experimental investigation of palm kernel shell and cow bone reinforced polymer composites for brake pad production. *International Journal of Chemistry and Material Research*, 2015,. 3(2), 27-40.

Moda, H. M., Sawyerr , H., & Clayson, A. What will go wrong has gone wrong: asbestos exposure risk among construction workers in Nigeria. *Policy and Practice in Health and Safety*, 2018, 1-12.

Ngwaba L.C and Aikhuele D.O. Development And Evaluation Of Asbestos-Free Brake Pads Produced From Costus Afer Waste And Local Gum Arabic. Journal of Mechanical Engineering and Technology (JMET), 2023; 15(1):11-24. DOI:10.54554/jmet.2023.15.01.002

Nicholson*Facts About Friction.* Croydon, PA: P & W Price Enterprises, Inc. 1995.

Nie, X., et al. Carbon-Carbon Composite Materials in Aviation Brakes: A Review." *Journal of Materials Science & Technology*, 2014, 30(5), 435-441.

Pinca-Bretotean C., Crăciun A.L., Josan A ., Ardelean M. Friction and wear characteristic of organic brake pads material, *IOP Conf. Ser.: Mater. Sci. Eng*., 2019, 477 012009. DOI: 10.1088/1757-899X/477/1/012009.

Purboputro P.I., Hendrawan A., Hariyanto A. Use of bamboo fiber as a brake pad lining material and the influence of its portion on hardness and durability. *IOP Conference Series Materials Science and Engineering*, 2018; 403(1):012100. DOI:10.1088/1757-899X/403/1/012100

Ramousse S., Høj J.W., Sørensen O. T. Thermal Characterisation of Brake Pads. Journal of Thermal Analysis and Calorimetry, 2001, 64(3). DOI: 10.1023/A:1011575013779

Rödelsperger, K., Jahn, H., Brückel, B., Manke, J., Paur, R., & Woitowitz, H. J. (1986). Asbestos dust exposure during brake repair. *Am J Ind Med*, 10(1), 63-72.

Sadhukhan A.K., Gupta P., Goyal T., Saha R.K. Modelling of pyrolysis of coal biomass blends using thermogravimetric analysis. *Bioresource Technology*, 2008; 99:8022-8026.

Yilma K.T., Tesfaye T., Enawgaw H., Ayele M., Limeneh D.Y., Gibril M., Kong F. Optimizing the Extraction of Keratin from Cattle Hoof Using Central Composite Design. *Adv. Mater. Sci. Eng.* (2022), https://doi.org/10.1155/2022/4866467.

Zephaniah, H. S., & Aremu, S. O. (2019). Asbestos: A Silent Potent Killer. *European Journal of Environment and Public Health*, 3(2), 1-7.